Evaluating the Sustainability of Electric Buses During Operation via Field Data

J Intel Connect Veh

Research Article

Evaluating the sustainability of electric buses during operation via field data

Baozhen Yao[1], Zhihao Qi[1], Ziqi Liu[2], Minke Zhu[2], Shaohua Cui[2,✉], Radu-Emil Precup[3,4], Raul-Cristian Roman[3]

Cite this article: Yao B Z, Qi Z H, Liu Z Q, et al. *J Intel Connect Veh* 2025, **8**(3): 9210061. https://doi.org/10.26599/JICV.2025.9210061

ABSTRACT: Environmental sustainability is a crucial issue for all human beings, and vehicle emissions significantly contribute to climate change. This has prompted many countries, including China, Norway, and Germany, to focus on electrifying transportation. This study quantifies the life cycle carbon dioxide (CO_2) emissions of electric buses (EBs) in Guangzhou, China, via a life cycle analysis methodology, revealing an average life cycle emission of 1,097.07 g CO_2·km^{-1}·vehicle^{-1}. The operation and charging stage contributes the most to the lifespan of CO_2 emissions at 69.6%, driven by carbon-intensive power grid. Compared with conventional internal combustion engine buses, EBs result in significant emission reductions, but regional grid carbon intensity variations across China mean that their benefits depend on nationwide green energy adoption. By 2030, emissions are projected to decline by 15.28%, aligning with carbon peak goals. The findings emphasize that transitioning to renewable energy grids and hybrid technologies is critical for sustainable transportation.

KEYWORDS: EBs; GHG emissions; life cycle analysis (LCA); electrification of transportation

1 Introduction

Our world is confronted with an unprecedented challenge in the realm of climate change. Research indicates that the global automotive sector, including transportation, accounts for up to 23% of global energy-related greenhouse gas (GHG) emissions, equivalent to approximately 8.7 Gt of carbon dioxide (CO_2) per year. Road vehicles are the largest contributors, representing approximately 70% of direct transportation emissions (Ritchie, 2020). In Europe, road vehicles also emit significant amounts of GHGs, particularly methane and nitrous oxide (Liu et al., 2024). Moreover, Japan is actively working to reduce its GHG emissions and has set ambitious carbon neutrality goals (Li et al., 2023). Across different regions, countries are introducing new policies to support the electrification of transportation and invest in improved charging infrastructure (Shui et al., 2024). The adoption of electric buses (EBs) in urban mass transit systems offers a promising opportunity to reduce fossil fuel consumption, GHG emissions, and pollution while enhancing the efficiency and sustainability of urban mobility (Koech and Fahimi, 2024). These policies reflect a global consensus on electrification as a pathway to decarbonization. However, the implementation of these policies varies significantly: Europe focuses on strict emission standards and grid decarbonization, Japan prioritizes technological self-sufficiency, and China leverages subsidies and infrastructure expansion. Despite these efforts, gaps remain in harmonizing policy objectives with operational realities. Nevertheless, existing studies on electric bus sustainability often overlook critical real-world complexities (Lin et al., 2025). For example, most life cycle analysis (LCA) models assume constant energy consumption rates and neglect variations caused by driving patterns, weather conditions, or infrastructure quality factors that significantly affect emissions and costs in practice. Moreover, while there are links between these policies, such as the shared goal of reducing emissions through electrification, they often operate independently without sufficient coordination.

Electric public transit systems also present significant challenges. EBs are already 2–4 times more expensive than conventional diesel buses (DBs). Moreover, EBs have secondary impacts on other systems, such as changes in grid demand and infrastructure requirements. They also face issues related to service availability and frequent battery replacements due to degradation. A key limitation of prior research is its heavy reliance on theoretical assumptions rather than empirical data. Similarly, service availability rates are frequently exaggerated because charging delays or maintenance downtime observed in cities with high EV adoption are underestimated.

These factors can significantly increase life-cycle emissions and energy consumption, which are highly dependent on real-world usage and charging pattern data that can be obtained through field operations. The studies concerning LCA of electric buses are either qualitative discussions or are based on strong consumption of the availability of EBs for service and the life spans of electric

[1] School of Mechanical Engineering, Dalian University of Technology, Dalian 116024, China. [2] Departmment of Architecture and Civil Engineering, Chalmers University of Technology, Gothenburg 41296, Sweden. [3] Department of Automation and Applied Informatics, Timisoara 300223, Romania. [4] Center for Fundamental and Advanced Technical Research, Romanian Academy-Timisoara Branch, Timișoara 300223, Romania.

✉ Corresponding author. E-mail: shaohuac@chalmers.se

Received: March 7, 2025; Revised: April 12, 2025; Accepted: April 22, 2025

Tsinghua University Press | Available on IEEE Xplore

buses and batteries without field data, which can result in biases to some extent. To resolve these biases, a case study of electric buses in Guangzhou is conducted for this thesis project, where the sustainability of electric buses during operation is evaluated via field data. The LCA is the main method for evaluating bus sustainability. Additionally, the performance of EBs under different ambient temperatures was also investigated. In this study, socioeconomic factors such as the cost of electric buses, changes in grid demand, and infrastructure needs also implicitly influence the outcome changes. In this study, the goal of LCA is to evaluate the GHG emissions of each stage of the entire life cycle of electric buses, namely, manufacturing, operation and end-of-life.

This study aims to conduct a quantitative life-cycle analysis on electric buses with field data in Guangzhou, China. Inventory data involving all the processes of an electric bus will be collected. Afterward, a customized assessment framework is developed to conduct a life-cycle analysis of electric buses, followed by a qualitative analysis of the influence of electrification of buses on power systems, real operation costs, and emissions. The last step is to identify the hot spot process that results in the most emissions during the life cycle and critical hurdles for sustainable development.

2 Literature review

2.1 Energy consumption of EBs

Sun et al. (2024) demonstrated that buses consume more energy under congested traffic conditions. This finding aligns with that of Eufrásio et al. (2023). By using dedicated bus lanes in traffic congestion, the energy consumption of both EBs and DBs can be lowered by up to 25% compared with regular traffic conditions for buses that are in shared-use bus lanes. These findings highlight the importance of the operational context in energy efficiency. Using specific energy consumption is a great way to evaluate the energy consumption of vehicles in general. The specific energy consumption is the energy consumption per km. In this way, the difference in the operational route can be offset. The average consumption of the two buses studied by Eufrásio et al. (2023) is 1.19 $kWh \cdot km^{-1}$ for one bus and 1.27 $kWh \cdot km^{-1}$ for the other, with a daily range of 0.94–2.29 $kWh \cdot km^{-1}$. Building on these empirical insights, Abdelwahab et al. (2024) proposed a comprehensive model to compute energy consumption, charging time, and state of charge (SoC). This approach integrates parameters such as battery capacity, driving distance, and charging station spacing, addressing gaps in previous studies that focused solely on static energy metrics. For example, by incorporating battery discharge rates and thermal dynamics, their model refines the estimation of minimum charging time constraints, thereby improving operational planning accuracy. Therefore, this research focuses on the accuracy and comprehensiveness of data related to the operation stage.

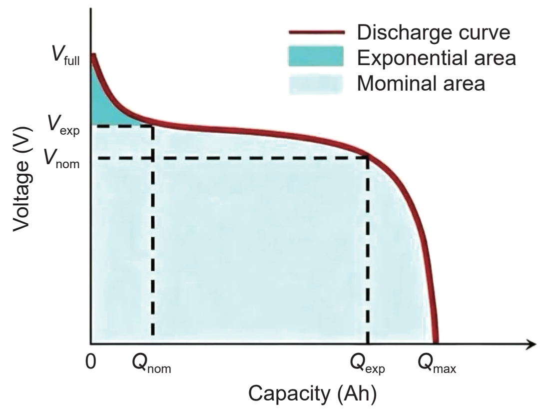

Fig. 1 Example of a typical battery discharge curve. Reproduced with permission from Karabacak et al. (2020), © Ilker Örs 2020.

2.2 Electrical vehicle (EV) batteries

Fig. 1 shows a typical battery discharge voltage curve (Karabacak et al., 2020). It is common for battery discharge to have a high discharge rate during the initial period; this phase is called the exponential area on a battery discharge curve. Within the nominal discharge area, the battery's power output is consistent as the voltage decreases steadily and stably. Toward energy depletion, the internal resistance of the battery increases; as a result, the voltage decreases drastically (Cui et al., 2025). This discharge behavior directly influences the battery lifespan and number of replacement cycles. For commercial EV batteries, degradation thresholds are standardized at 80% of the nominal capacity (Chen et al., 2022). The relationship between the discharge time and discharge rate at a certain capacity is described by Eq. (1) (Liu et al., 2023):

$$t = H\left(\frac{C}{IH}\right)^k \tag{1}$$

where t (h) is the time taken during discharge, H (h) is the nominal discharge time in hours, C (Ah) is the nominal capacity, I (A) is the discharge current, and k is the Peukert constant.

Currently, 2 types of batteries (Table 1) are generally used in pure electric vehicles: ternary lithium-ion batteries (NMCs) and lithium-iron $LiFePO_4$ phosphate batteries (LFPs). Currently, NMC is the dominant battery type used in electric transportation (Fallah and Fitzpatrick, 2023). One leading reason is that NMC is lighter than the $LiFeO_4$ battery (LFB) in weight, making it more portable than its main competitor. Additionally, the energy density of NMC is generally approximately 190–260 $Wh \cdot kg^{-1}$, which is much greater than that of LFP, which is only approximately 90–130 $Wh \cdot kg^{-1}$. Although LFP is still a very competitive alternative, as LFP is considerably less expensive than NMC and is even a better choice in the long run, as outside of the mutually toxic element lithium, NMC batteries also contain critical elements such as cobalt, which is also a toxic heavy metal. In addition, LFP is much safer than NMC, as the burning point of NMC is approximately 350 °C, while LFB temperatures are much

Table 1 EV battery life-cycle CO_2 emissions from different studies

Type of battery	Region	Emission	Unit	Source
NMC811	China	91.21+154.1+2.68	kg CO_2-eq·kWh^{-1}	Chen et al. (2022)
Li-ion	—	22	kg CO_2-eq·kg^{-1}	Majeau-Bettez et al. (2011)
Li-ion	Europe	6	kg CO_2-eq·kg^{-1}	Notter et al. (2010)
Li-ion	USA	9.6	kg CO_2-eq·kg^{-1}	Li et al. (2023)
Li-ion	China	0.158–44.59	kg CO_2-eq·kg^{-1}	Li et al. (2023)

Note: Global averages mask regional disparities in electricity grids and recycling infrastructure.

higher at approximately 740–910 °C, and NMC tends to have greater temperature fluctuations during charging and discharging. Fallah and Fitzpatrick (2023) also reported that retired LFPs have advantages over NCMs on a second life, particularly in regions where renewable energy integration is limited but grid stability is critical for urban mobility systems. This finding aligns directly with the research subject of optimizing lifecycle emissions for electric buses in Guangzhou. Majeau-Bettez et al. (2011) and colleagues calculated GHG emissions of 22 kg CO_2 (eq·kg^{-1}) from Li-ion batteries. Li et al. (2023) reported that the global warming potential (GWP) and cumulative energy demand (CED) of recycling 1 kg spent lithium-ion phosphate batteries (LiBs) are 0.158–44.59 kg CO_2-eq and 3.3–154.4 MJ, respectively. These distinctions underscore the need for region-specific battery selection criteria. These findings indicate that carbon emissions during the lifespan of batteries are significant and cannot be ignored, especially in countries where electricity production relies heavily on fossil resources.

3 Methodology

The entire method (Fig. 2) is built around a cradle-to-grave LCA on an EB, which includes two main parts: the LCA process and operation data analysis.

3.1 LCA

LCA is a comprehensive method for evaluating the environmental impact of a product throughout its entire life cycle. This approach is particularly valuable in the energy sector. The framework of a general LCA is shown in Fig. 3 (Hauschild et al., 2018).

In this study, a cradle-to-grave LCA is conducted, i.e., from raw material extraction to disposal. This is crucial for e-buses where impacts are not only operational but also substantial in the production and disposal stages, especially considering electricity generation and battery manufacturing and disposal. The life cycle of an EB is usually divided into the following processes: electricity generation and transformation, raw material extraction and transportation, operation and charging electricity, and end-of-life. Specific processes are explained in Section 3.1, i.e., system boundaries and life cycle inventory (LCI) analysis.

The selection of the LCA for this study is based on several key advantages. First, LCA provides a holistic view of the environmental impacts across all stages of the electric bus life cycle, allowing for a comprehensive assessment that includes not only the operational phase but also the often-overlooked production and disposal stages. This is particularly important for electric buses, as the environmental impact of battery production and disposal can be significant. Second, LCA enables the comparison of different energy sources and technologies, which is essential for understanding the overall environmental footprint of electric buses in the context of the local energy grid.

However, it is important to acknowledge the limitations of the LCA method. One limitation is the data requirements; accurate

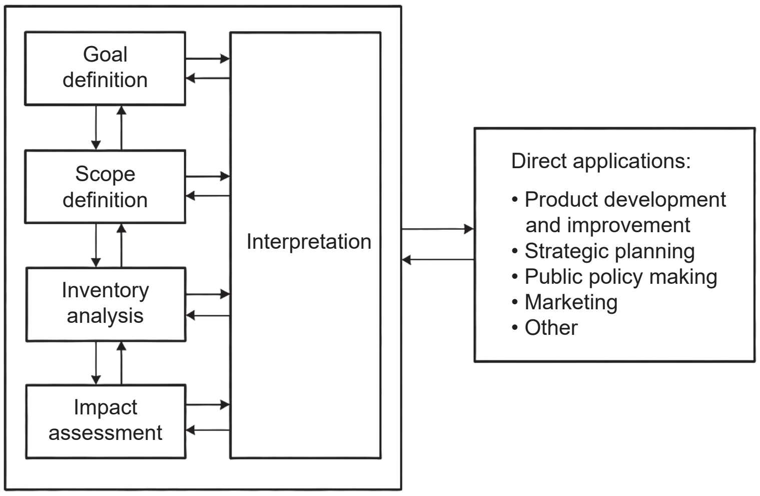

Fig. 3 Framework of the LCA modified from the ISO 14,040 standard. Reproduced with permission from Hauschild et al. (2018), ©Springer International Publishing 2018.

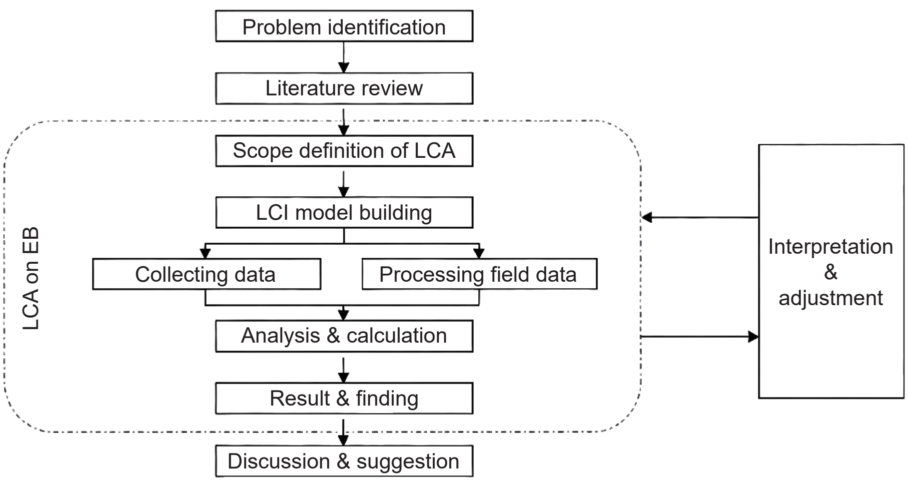

Fig. 2 Framework of the methodology used in this study.

清華大学出版社 Tsinghua University Press | Available on IEEE Xplore

and comprehensive data are needed for each stage of the life cycle, which can be challenging to obtain, especially for emerging technologies such as electric buses. Additionally, LCA models can be complex and require significant computational resources, which may limit their accessibility and ease of use. Furthermore, the results of LCA can be sensitive to assumptions about future technological developments and changes in the energy mix, which may affect the long-term accuracy of the findings.

Despite these limitations, LCA remains the most suitable method for evaluating the environmental impact of electric buses in this study because of its comprehensive nature and ability to provide a detailed understanding of the full life cycle impacts.

The goal of this LCA is to evaluate the sustainability of EBs. To quantify sustainability, the environmental impact category needs to be fixed. Greenhouse gas emissions from vehicles are among the most significant environmental impacts contributing to climate change. CO_2 emissions are selected as the quantitative indicator for this study. The following specific questions are researched: (1) How much CO_2 emission will be emitted during the life cycle of an EB operating in Guangzhou, China, on the basis of field data. (2) Which process in the life cycle has the highest emission. (3) How do these factors, such as the assumed local power grid and temperature, affect the CO_2 emissions of an EB. The overall intention is to provide a quantitative evaluation of the emissions of EBs for the study of their environmental impact, strategic planning of public transportation, and further adjustment of the energy grid aimed at electrification and the net zero strategy. The intended audience includes bus manufacturers, public transportation operation companies, government decision-makers, and environmental organizations.

When conducting LCA, it is critical to select an appropriate functional unit. Three functional units are commonly used when the assessment objective is an EB: impact per kilowatt-hour battery, impact per km battery, and impact per km the EB drives. Since the aim is to evaluate the EB's sustainability performance instead and the field data for analysis are focused on the operation stage instead of the battery, the impact per km is selected as the functional unit in this study, i.e., the grams of CO_2 emitted per km per EB.

Since all the buses analyzed are still at the service of public transportation, no monitored data of a lifetime driving distance are accessible. Given the estimated lifespan (by the number of years) of an EB (L), the total length of all routes (L_{tot}) using km as the unit, the number of buses in operation, the number of shifts per route per day (N_{shifts}), and the approximate lifespan of an EB, the lifetime driving distance of one EB can be calculated via Eq. (2). The number of buses is given by N_{buses}.

$$\text{TotalKilometersperBus} = \frac{365 L L_{\text{tot}} N_{\text{shifts}}}{N_{\text{buses}}} \tag{2}$$

In addition to the technical and environmental aspects, socioeconomic factors play a crucial role in the overall sustainability assessment of electric buses (Liu et al., 2023). These factors include the costs associated with electric bus procurement, operation, and maintenance, as well as the impact on grid demand and the requirements for supporting infrastructure. Studies have shown that the transition to electric buses can lead to a higher total cost of ownership because of significant investments in buses and charging infrastructure (Sistig et al., 2025). Additionally, the limited range of electric buses can increase the need for additional vehicles and drivers, further affecting operational costs. These socioeconomic considerations are essential for understanding the feasibility and impact of electric bus systems in real-world applications.

The system boundaries refer to the scope of the LCA. The technical boundary is built on the basis of a literature review and is shown in Fig. 4. The temporal boundary refers to the lifespan duration of an EB. The selection of CO_2 as the core indicator is further justified by Guangzhou's electricity mix: as of 2022, coal-fired power accounted for 52% of the city's grid energy, making CO_2 emissions highly sensitive to grid decarbonization progress. This context underscores the necessity of region-specific emission factors in life cycle analysis.

The 8-year service life for EBs in Guangzhou is guided primarily by local regulatory requirements. According to the Guangzhou Municipal Public Security Bureau Traffic Police Detachment Vehicle Management Office (2018), heavy-duty vehicles (including electric buses) operating with > 20 seats must

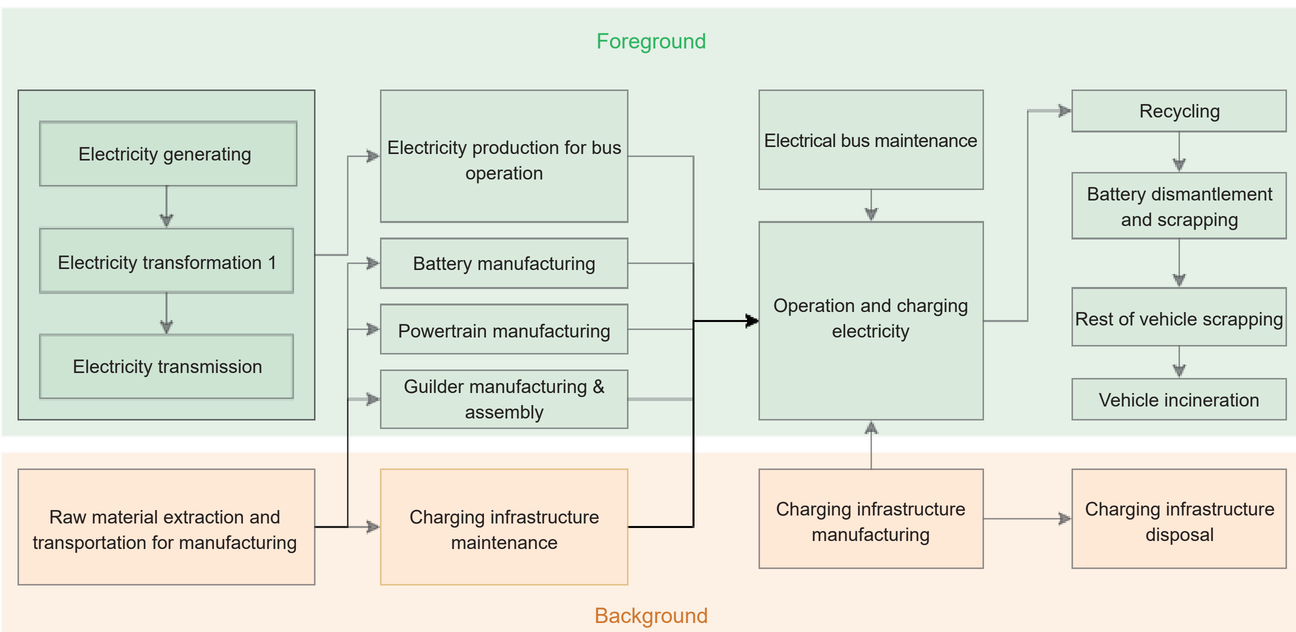

Fig. 4 Initial flowchart.

undergo mandatory scrapping after 8 years of service to align with provincial air quality improvement targets. This regulation reflects Guangzhou's accelerated phase-out strategy for aging vehicles, which is stricter than the national average lifespan of 12 years for diesel buses.

To frame the technical boundaries, the foreground and background are set to differentiate between the processes that are directly controlled or influenced by the decision-makers of the product system being studied (foreground) and those that are not (background). In the foreground, the assessment begins with the generation and further processing of electricity, manufacturing bus components and assembling. Afterward, there is operation charging and maintenance of the bus itself. Additionally, end-of-life scenarios are considered, featuring recycling processes, battery dismantlement, and vehicle scrapping. This foreground analysis is critical because it captures the direct emissions and energy usage associated with the active service life of electric buses. The background processes provide context for the support systems that indirectly contribute to the life cycle of EBs. This includes the raw material extraction and transportation required for manufacturing bus components and batteries and the creation of charging infrastructure. These stages are imperative for understanding the cradle-to-grave environmental impacts of the system. Buses usually have a 12-year service life before being eliminated. However, this study refers to the local regulation on vehicle service life by the Guangzhou Municipal Public Security Bureau Traffic Police Detachment Vehicle Management Office (2018), where vehicles with or with more than 20 seats, operating vehicles to nonoperating vehicles, or nonoperating vehicles to operating vehicles, are usually in operation for 8 years. Given that and following the form of a time frame in LCA from Hauschild et al. (2018), the time frame for this LCA is shown in Fig. 5. The adoption of Hauschild et al.'s (2018) time frame approach is based on its dynamic alignment with policy-driven lifecycle phases. This framework allows us to isolate direct emissions from regulated operational activities while accounting for indirect, long-term impacts through sensitivity analyses.

Inventory analysis is a crucial aspect of life cycle assessment and involves the collection and compilation of data on elementary flows from all processes in a product system. It starts by identifying unit processes of the product system and then collecting data. With the needed data available, the LCI model is constructed, and calculations are conducted.

On the basis of the initial flowchart (Fig. 4) and further literature reviews, the identified unit processes of an EB, i.e., stages in the life cycle, include powertrain manufacturing, battery manufacturing, glider manufacturing and assembly, operation and charging electricity, and end-of-life.

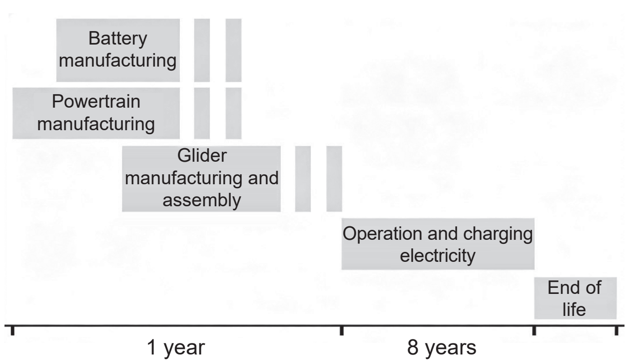

Fig. 5 Time frames for different life cycle stages. Reproduced with permission from Hauschild et al. (2018), © Springer International Publishing 2018.

The inventory data collection involves gathering information on all the inputs (e.g., raw materials, energy) and outputs (e.g., emissions, waste) associated with each stage of the life cycle. The data used in this study were collected from two sources. Data on the operation and charging of electricity are extracted from field data collected from sensor monitoring of buses in Guangzhou, China. The rest are from local governmental disclosure and academic studies.

This study collects numerical data at the unit process level (e.g., battery, powertrain, and glider manufacturing), with inputs including energy, raw materials, and components, and outputs comprising products, byproducts, and CO_2 emissions (Table 2). CO_2 emissions are critical for environmental impact assessment, whereas intermediate outputs (e.g., battery packs and scrapped EBs) serve as inputs for subsequent processes in the life cycle analysis.

As previously mentioned, data on the operation and charging electricity are from sensor monitoring of the buses. This study utilizes comprehensive field data from more than 500 buses in 2021, detailing bus charging, location, operation, etc. Specifically, charging data—including timestamps, battery SoC, charging status, count, and station location—are analyzed to estimate energy consumption. Details about data wrangling and processing are presented in Section 3.2. For the total lifespan operation distance, because the current EBs are still in operation and not yet disposed of, it is calculated with the raw data collected and through Eq. (2), which has already been justified in Section 3.1. According to the local public transportation app, the average number of shifts of one bus route per day is 96. The length of all bus routes is 23,000 km, while the total number of buses is 15,000 vehicles. Since Guangzhou city has achieved 100% electrification with respect to public buses, these numbers are applicable for this study, especially for EBs. Given this, the lifespan operation can be calculated via Eq. (3):

$$\begin{aligned}\text{LifespanOperation} &= \frac{365LL_{\text{tot}}N_{\text{shifts}}}{N_{\text{buses}}} \\ &= \frac{365\times 23000\times 96\times 8}{15000} = 429824 \quad (3)\end{aligned}$$

The rest of the inventory data are from other research or governmental disclosure. Table 3 shows the data sources and values that were used. Initial normalization for values here has already been conducted.

Fig. 6 presents a simplified unit process in which battery manufacturing is used as an example. Two primary inputs are shown: electricity (used for manufacturing) and materials. The output first includes a completed battery pack, which is ready for further processes, i.e., glider manufacturing and assembly. Materials losses are another output that needs to be considered, inevitably from inefficiencies during manufacturing. Additionally, the process generates emissions of CO_2 directly from electricity used for manufacturing and indirectly from material extraction. The qualitative relationships among all the inputs and outputs are shown in Eqs. (4) and (5):

$$\text{Materialsmass}_{\text{input}} = \text{Mass}_{\text{Batterypack}} + \text{Mass}_{\text{losses}} \quad (4)$$

$$\text{CO}_{2\text{output}} = \text{CO}_{2\text{Materialextraction}} + \text{CO}_{2\text{Electricityuse}} \quad (5)$$

Here, a highly critical indicator is the emission factor (EF). It relates the quantity of a pollutant released to the atmosphere with the activity causing the release. The context of electricity (Eq. (6)) refers to the quantitative relationship between electricity

Table 2 Identified inputs and outputs for each unit process

Unit process	Input	Output
Battery manufacturing	Material	CO_2 emission
	In battery	From cell materials
	In other parts of battery pack	From other materials
	Losses	From electricity use
Battery manufacturing	Electricity	Battery pack
	For cells	Wasted materials
	For others	—
Powertrain manufacturing	Material	CO_2 emission
	Materials in powertrain	From materials
	Material losses	From electricity use
	Electricity	Electric powertrain
	—	Wasted materials
Glider manufacturing and assembly	Battery pack	CO_2 emissions
	Electric powertrain	From materials
	Glider, materials	From electricity use
Glider manufacturing and assembly	In glider	EB
	Losses	Wasted materials
	Electricity	—
Operation and charging electricity	EB	CO_2 Emission
	Charging electricity	From electricity use
	—	Scrapped EB after operation lifespan
End of life	EB, preparation of recycling	CO_2 emissions
	Battery, dismantled, and scrapped	From electricity use
	Rest of EB scrapped	From incineration
	Share of EB for incineration	—
	Shredding, refining, and sorting	—

generation or consumption and carbon emissions (Yang et al., 2023). This study used predicted EFs for China's southern grid in 2021, derived from models established in the referenced paper via statistical analysis of fossil fuel-fired power generation data from 2006–2019 (Zhang et al., 2023). The selection of EFs in this study is based on the need for accurate and up-to-date data that reflect the current and future trends of China's energy grid. The predicted EFs are used to account for the evolving nature of the grid, which is crucial for assessing the long-term environmental impact of electric buses.

$$\text{EmissionFactor}_{\text{Electricity}} = \frac{\text{Emission}}{\text{Electricity consumption}} \tag{6}$$

Therefore, the total CO_2 emissions in the battery manufacturing stage can be written as Eq. (7):

$$\begin{aligned}\text{CO}_{2\text{Battery Manu.}} &= \sum_{\text{source}=1}^{n} \text{EnergyuseEF} \\ &= \text{Mass}_{\text{Cell materials}}\text{EF}_{\text{Extraction}} \\ &\quad + \text{Mass}_{\text{Other materials}}\text{EF}_{\text{Extraction}} \\ &\quad + \text{ElectricityEF}_{\text{Electricity consumption}}\end{aligned} \tag{7}$$

Summing the five identified unit processes and inputs/outputs of each process, the life cycle of the EB is connected and shown in Fig. 7. Using the same method, the quantification formulas of emissions for the other four stages can also be modeled via Eqs. (8)–(11). The emissions of all five processes are summed via Eq. (12).

$$\begin{aligned}\text{CO}_{2\text{Powertrain Manu}} = {} & \text{Mass}_{\text{Materials}}\text{EF}_{\text{Extraction}} \\ & + \text{ElectricityEF}_{\text{Electricityconsumption}}\end{aligned} \tag{8}$$

$$\begin{aligned}\text{CO}_{2\text{Giler Manu. Assembly}} = {} & \text{Mass}_{\text{Materials}}\text{EF}_{\text{Extraction}} \\ & + \text{ElectricityEF}_{\text{Electricityconsumption}}\end{aligned} \tag{9}$$

$$\text{CO}_{2\text{Operationandchargingelectricity}} = \text{ElectricityEF}_{\text{Electricityconsumption}} \tag{10}$$

$$\begin{aligned}\text{CO2Endoflife} = {} & \text{Mass}_{\text{Materials}}\text{EF}_{\text{incineration}} \\ & + \text{ElectricityEF}_{\text{Electricityconsumption}}\end{aligned} \tag{11}$$

$$\begin{aligned}\text{CO}_{2\text{Lifecycle}} = {} & \text{CO}_{2\text{PowertrainManu.}} + \text{CO}_{2\text{GilerManu.\&Assembly}} \\ & + \text{CO}_{2\text{Operationandchargingelectricity}} + \text{CO}_{2\text{Endoflife}}\end{aligned} \tag{12}$$

Understanding the environmental implications of adopting electric bus systems is pivotal. Impact analysis involves categorizing and quantifying sustainable impacts via inventory data. As mentioned above, the primary focus on impacts is on CO_2 emissions. What follows is to calculate the emissions, convert them into the set functional unit, and then interpret these results, including comparisons and source analysis.

Comparing the environmental impact of EBs and conventional internal combustion engine (ICE) buses is crucial in the transportation industry (Koech et al., 2024). Therefore, a discussion of this topic will focus on analyzing the sustainability of these two modes of transportation, particularly in terms of their

Table 3 Data values and sources

Data	Value	Unit	Source
Battery manufacturing			
Materials	1.648	ton·batt^{-1}	Summation of materials in battery and losses
In battery	1.200	ton·batt^{-1}	China buses (2024)
In other parts of battery pack	0.400	ton·batt^{-1}	
Losses	(3%) 0.048	ton·batt^{-1}	
Electricity			Nordelöf et al. (2019)
For cells	15.000	kWh·kg^{-1}	
For others	1.000	kWh·kg^{-1}	
Powertrain manufacturing			
Materials	0.412	ton·pwt^{-1}	Summation of materials in powertrain and losses
Materials in powertrain	0.400	ton·pwt^{-1}	Guangzhou Municipal Public Security Bureau (2018)
Material losses	(3%) 0.012	ton·pwt^{-1}	Nordelöf et al. (2019)
Electricity use in factory	5.000	kWh·kg^{-1}	
Glider manufacturing and assembly			
Battery pack	2.000	batt·veh^{-1}	Set by LCA
Electric powertrain	1.000	pwt·veh^{-1}	
Glider, materials	7.745	ton·veh^{-1}	Summation of materials in glider and losses
In glider	7.000	ton·veh^{-1}	China buses (2024)
Losses	(3%) 0.475	ton·veh^{-1}	Nordelöf et al. (2019)
Electricity	0.470	kWh·kg^{-1}	—
Operation and charging electricity			
Operation Lifetime	8	year	Guangzhou Municipal Public Security Bureau Traffic Police Detachment Vehicle Management Office (2018)
Total length of all bus routes	23,000.000	km	Daily (2021)
Number of buses in operation	15,000.000	No. of buses	
Numbers of shifts perroute per day	96.000	No. of shifts	Guangzhou Local Information (2024)
Charging electricity,,including charger losses	132.700	kWh·veh^{-1}·day^{-1}	
From Electricity	0.8475	kg CO_2	Zhang and Xu (2023)
Use (China South Grid)		eq.·kWh^{-1}	
End of Life			
Vehicle, preparation of recycling	1.000	veh	Set by LCA
Battery, dismantled, scrapped	2.000	batt·veh^{-1}	
Share of vehicle, incineration	0.15%	—	Nordelöf et al. (2019)
Shredding, refining and sorting	1.000	kWh·kg^{-1}	—

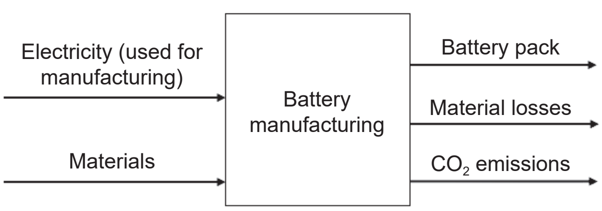

Fig. 6 Simplified unit process of battery manufacturing. Reproduced with permission from Nordelöf et al. (2019), © Elsevier 2019.

CO_2 emissions. Additionally, inspired by the literature review, this analysis examines and interprets how factors such as the power grid and temperature can influence the sustainable performance of electric buses.

3.2 Bus operation field data analysis

Three sets of field data were used in this study, all from May 2021 in the city of Guangzhou, China. In total, there are 1,048,576 data entries. The scopes of the datasets are shown in Figs. 8 and 9.

The first 2 datasets are the controller area network (CAN) and GPS data of 500 buses on May 1, 2021; a data sample for both the bus CAN and the GPS can be found in Tables 4 and 5. These 2 sets of data have a larger time gap between data input points, and they are used to understand the general operational behavior of buses, such as the operation time, break time, and number of trips per day, and to calculate the average energy consumption of different buses.

The third dataset contains bus No. 497's CAN and GPS operation data for all days in May 2021. The data are read and logged every second during all the trips recorded in this dataset. Since the temperature range is quite wide during this month, this dataset is used to understand the impact that the ambient temperature has on battery performance, energy consumption and bus operation. An example of this dataset and more information on the analysis process for the impact of ambient temperature can be found in Section 4.2.

Tsinghua University Press | Available on IEEE Xplore

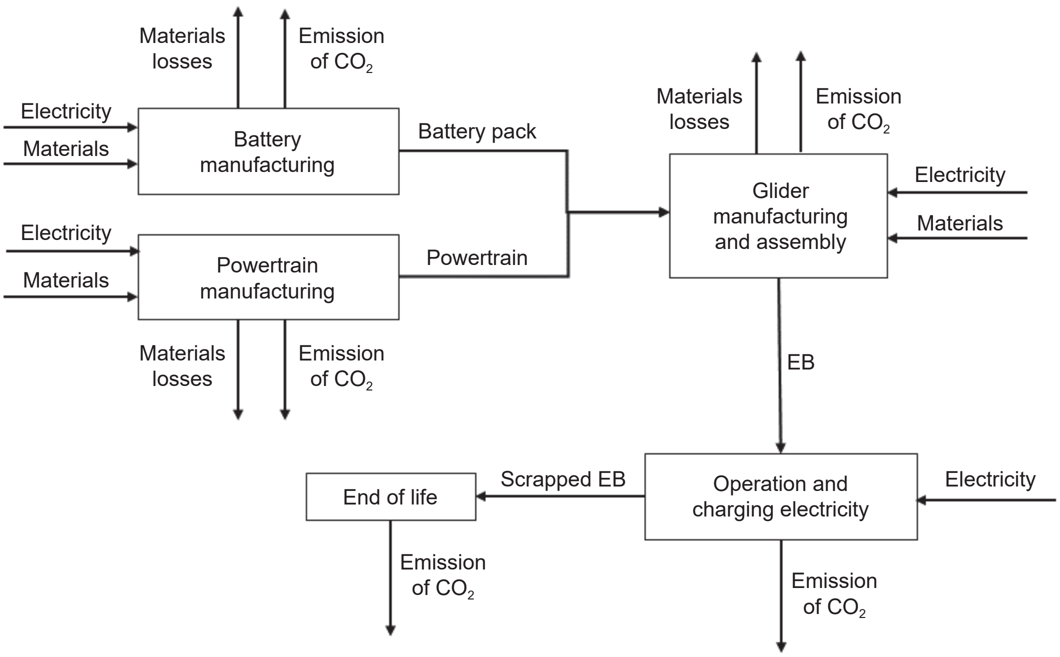

Fig. 7 Simplified unit processes connected. Reproduced with permission from Zhang and Xu (2023), © Elsevier 2023.

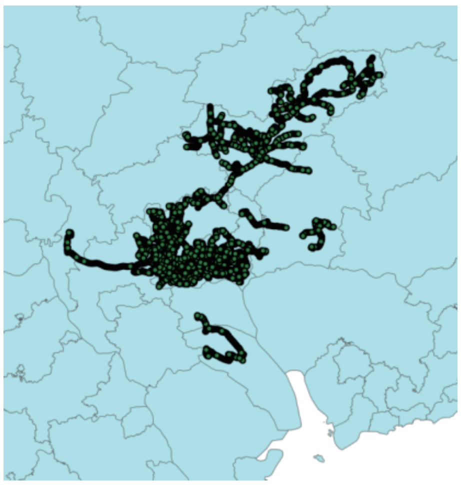

Fig. 8 Scope of the bus routes included in the data.

Fig. 9 Scope of the data.

Both sets of field data used in this study have extensive information on bus charging, location/GPS, departing station and terminal station, bus operation (speed, speed on wheel, total mileage, total voltage, total current, operation time, running mileage, running duration, single trips' beginning and ending time, service type, etc.), inside and outside temperature, route, direction, component status and gears.

Following the aim and scope of this study defined in Section 1, the objective data for the bus operation analyses included the bus ID, data input time stamp, SoC, charging status, speed, total voltage, total current, total mileage, GPS mileage, service type and operation time. These data were extracted and ordered by bus ID as the primary sorting criterion and the time stamp of the data input point as the secondary sorting criterion. Bus temperature and component status are considered factors in the LCA process.

The total mileage was read directly from the odometer on the buses. This and the GPS mileage were used to estimate the lengths of different bus trips. Although the exact length of these trips could not be calculated, as the odometer only reads integers in kilometers, only the point-to-point distance could be calculated with GPS mileage data.

Table 4 CAN data sample of 3 buses on May 01, 2021

Bus ID	51	100	119
Time stamp	18:12:48	14:39:58	12:12:42
SoC (%)	40	67	70
Charging status	00	00	00
Speed (km·h^{-1})	16.834	15.001	0.000
Total mileage (km)	27,836	15,089	15,312

Different bus service types (round trips, one-way routes, short routes, breaks, first/last trips, and fast routes) significantly impact traffic congestion simulations and energy consumption analysis. Fast routes, operating on highways/dedicated lanes with minimal congestion and traffic signals, reduce braking/acceleration and lower overall energy use. The first trips start with 100% battery charge (overnight charging), minimizing initial energy loss. Conversely, last trips experience slightly higher energy consumption due to battery aging and lithium-ion battery kinetics: faster discharge/charge rates occur at the start and end of typical battery cycles (Fig. 1), aligning with daily trip start/end phases. This classification directly links service type characteristics to traffic intensity and battery states for precise energy modeling.

Table 5 GPS data sample

Bus ID	Triplog ID	Duration	Trip mileage (km)	Begin	End
1	914 876 697	12	3	11:53:00	12:05:00
1	915 010 112	16	2.6	17:35:00	17:51:00
1	915 026 658	15	2.6	18:35:00	18:50:00
…	…	…	…	…	…
500	914 786 308	38	19.11	08:30:00	09:08:00
500	914 813 553	45	20.52	09:10:00	09:55:00

Table 6 Charging status reference and the corresponding statuses

Charging status reference	Charging status
00	Not charging
01	Charging
02	Charging finished
03	Charging stopped

Specifically, the data on bus charging, which consists of the data input time, SoC in the battery pack, charging status, bus charge count and location of the charging station, are used to calculate/estimate the energy consumption in this study; more details are discussed in Section 3.2. There are 4 different charging statuses in the data, and they refer to different charging scenarios, as listed in Table 6. This information was used to better determine how many times the buses were charged through a 24-h window.

The speed and SoC against time-bus operational graphs were plotted first. Outliers can often be found in the dataset, as the sensors on the buses have limited accuracy during operation; hence, singular outliers were removed by removing data points that make the SoC curve gradient inconsistent in Python. Data entries that contained too many outliers or more than a few hours of no data input were excluded from further investigation. In total, 125,801 data entries were removed, which left 922,775 data entries for the rest of the study.

An example of the operational graph of bus No. 237 on May 1, 2021, can be found in Fig. 10. Before data cleaning (Fig. 10a), an obviously inconsistent data outlier that misreads the SoC as 0% can be found at approximately 6:00, causing the SoC curve to suddenly drop. After the data outliers are removed, as shown in Fig. 10b, a smooth decrease in the SoC curve, which indicates consistent energy consumption during bus operation, is obtained.

The speed of the buses was included in the graphs to determine how many trips and breaks they took during a 24-hour period. Additionally, these data help identify whether the bus was charged during breaks, which is crucial for accurately calculating energy

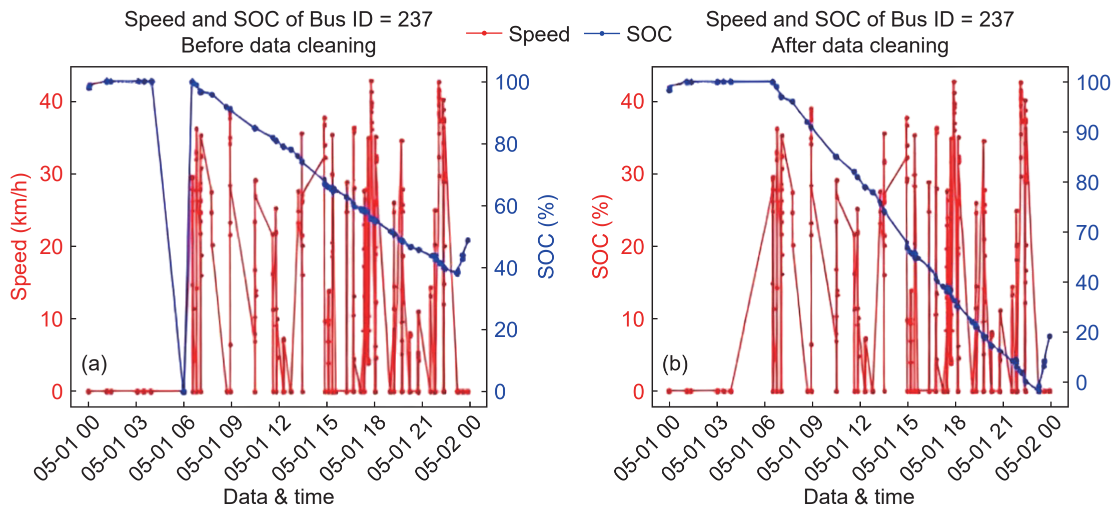

Fig. 10 Example of the operational graph of bus No. 237 on May 1, 2021.

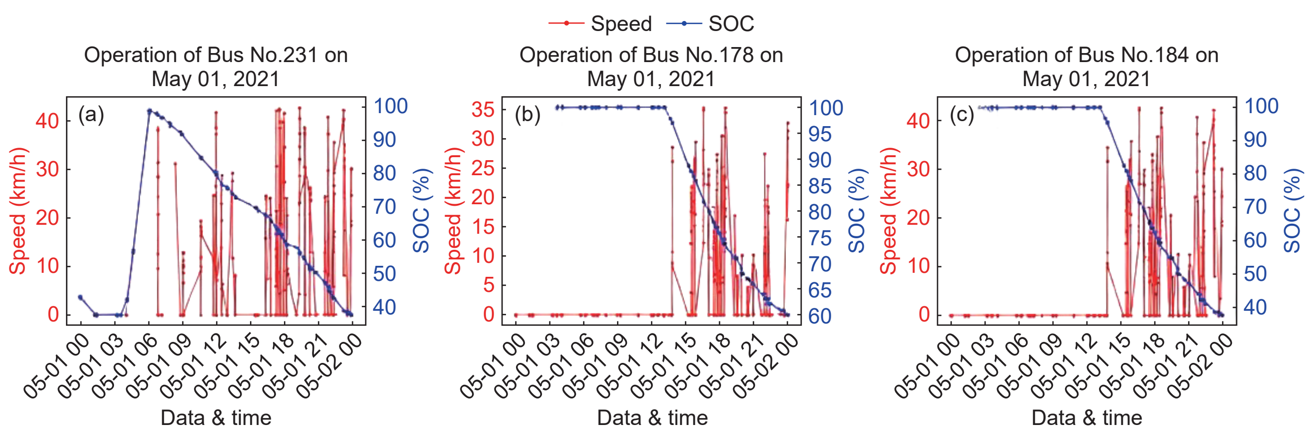

Fig. 11 Operation of buses on May 01, 2021.

https://doi.org/10.26599/JICV.2025.9210061

consumption. Taking bus No. 231 as an example, as shown in Fig. 11a, it can be easily seen from the speed information (red lines) that the bus had been charging from 03:00 to 06:00 overnight before driving out for its first trip in the morning from 09:00 to 12:00. The bus then took a break from 12:00 to 15:00 while being charged at the charging station, causing the SoC (blue curve) to rise from 65% to 100%.

Bus No. 178 is an example of one bus running a long trip without taking breaks or intermediate charging throughout 24 h, as shown in Fig. 11b. Bus No. 184 in Fig. 11c is an example of a bus taking one break (13:30–15:30) without being charged.

As previously mentioned in Section 3.2, there are 3 general types of bus operations. In the first type, the bus is charged overnight and only overnight and then continues to operate without breaks until the last trip of the day. In the second type, the bus is charged overnight and only overnight; it breaks during the day without charging until the last trip of the day. In the third type, the bus is charged overnight but also during break time in operation (Fig. 11a).

If the bus operates within the scope of the first 2 types, then its daily energy consumption is calculated via Eq. (13): $\mathrm{SoC}_{\mathrm{final}}$—the SoC in the battery pack at the end of the recorded trip (%), $\mathrm{SoC}_{\mathrm{intial}}$—the initial SoC in the battery pack at the start of the trip (%), and Q_{nom}—the nominal battery capacity (kWh).

$$E_{\mathrm{consumption}} = \frac{\mathrm{SoC}_{\mathrm{initial}} - \mathrm{SoC}_{\mathrm{final}}}{100} Q_{\mathrm{nom}} \tag{13}$$

If the bus can be categorized into the third operation type, then the extra charging times must be taken into consideration, as simply using the final and initial SoC to calculate the energy consumption will ignore the extra energy being charged into the battery. For this type, the bus's daily energy consumption is calculated via Eq. (14):

$$E_{\mathrm{consumption}} = \frac{\sum_{n=1}^{i} (\mathrm{SoC}_{\mathrm{initial}_i} - \mathrm{SoC}_{\mathrm{final}_i})}{100} Q_{\mathrm{nom}} \tag{14}$$

The 3 most common EV bus models in operation in the city of Guangzhou are the HUNAN CSR TIMES TEG6129 12-m pure electric city bus, the BYD Auto GZ6122LGEV2 electric bus, and the CRRC TEG6129BEV11 electric bus. The nominal battery capacity of these models can be found on the official website of Guangzhou Municipal Public Security Bureau (2018) and is listed in Table 7. Since the nominal battery capacities for these 3 models are similar, this study is performed under the assumption that all buses have a nominal battery capacity of 337.1 kWh.

The trip log of bus No. 178 in Fig. 11 is taken as an example to calculate its energy consumption on May 01, 2021. In this particular trip, the bus took only one trip in the 24-h window from 12:00–24:00, with a rather consistent decrease in the blue SoC curve, indicating a smooth journey. Upon the start of the trip, the bus had an initial SoC of $\mathrm{SoC}_{\mathrm{initial}}$ = 100%. The SoC then gradually decreased to 60% at 24:00. The energy consumption of this trip can then be obtained through Eq. (15):

$$E_{\mathrm{busid=178}} = 337.1 \times \frac{100 - 60}{100} \times 134.84 \tag{15}$$

The graph of energy consumption of this bus is shown in Fig. 12.

Table 7 Nominal battery capacity of the 3 major models of EBs in Guangzhou

Brand	Model	Nominal battery capacity (kWh)
HUNAN CSR TIMES	TEG6129	333.70
BYD AUTO	GZ6122LGEV2	337.71
CRRC	TEG6129BEV11	340.00

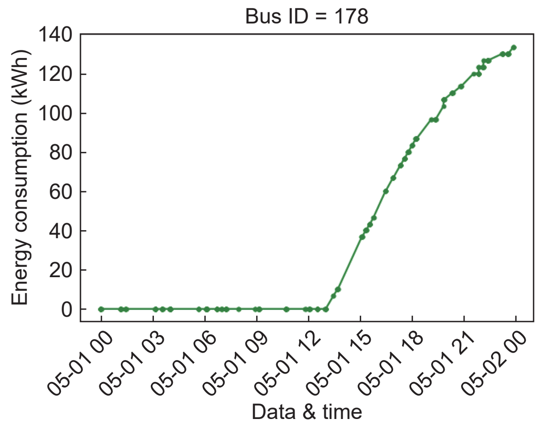

Fig. 12 Energy consumption graph of bus No. 178 (Guangzhou Municipal Public Security Bureau, 2018).

Equations (13) and (14) were used to calculate the daily energy consumption of all 500 buses during May 2021. The average energy consumption of these buses is 132.7 kWh. The average mileage per triplog ID for all 500 buses can be calculated by simply performing an average over all run_mileage (km), and the result is 132.7 kWh. The same is true for the average trip duration. The average mileage per day per bus can be calculated by adding the mileage of all trips logged for the same bus ID, and the result is 15.23 km. The average mileage per day per bus is 110.9 km. Finally, the average specific energy consumption for all buses can be calculated via Eq. (16), which yields a value of 1.197 kWh·km^{-1}.

$$E_{\mathrm{cons\_per\_km}} = \frac{E_{\mathrm{consumption}}}{\mathrm{run\_mileage}} = \frac{132.7}{110.9} = 1.197 \tag{16}$$

4 Results and discussion

4.1 Results

Table 8 below shows the lifetime environmental impact results, i.e., CO_2 emissions, for the EB's life cycle. Fig. 13 shows the emissions from each stage more visually. The operation and charging electricity process contributes the most to the overall lifespan CO_2 emission of an EB, at 764.02 g CO_2·km^{-1}, accounting for 70% of the overall emissions. This value is much greater than the sum of all three manufacturing processes, which is 311.74 g CO_2·km^{-1}. This strongly pinpoints where sustainability efforts should be made. The secondary hot spot is battery manufacturing, with a value of 202.19 g CO_2·km^{-1}, even though it accounts for only 18%. Considering the significant emissions from the operation stage, reflecting those important input data, the primary data for electricity consumed by EBs are from field data, the lifetime operation distance is based on a calculation based on public transportation information, and the EF for the local grid is obtained from model prediction for academic research.

4.2 Discussion

Given the CO_2 emissions of an EB and the identification of the

Table 8 CO_2 emissions in each life cycle stage

Process	Emission (g CO_2·km^{-1}·veh^{-1})
Battery manufacturing	202.19
Powertrain manufacturing	11.61
Glider manufacturing and assembly	97.94
Operation and charging electricity	764.02
End of life	21.31
Total	1,097.07

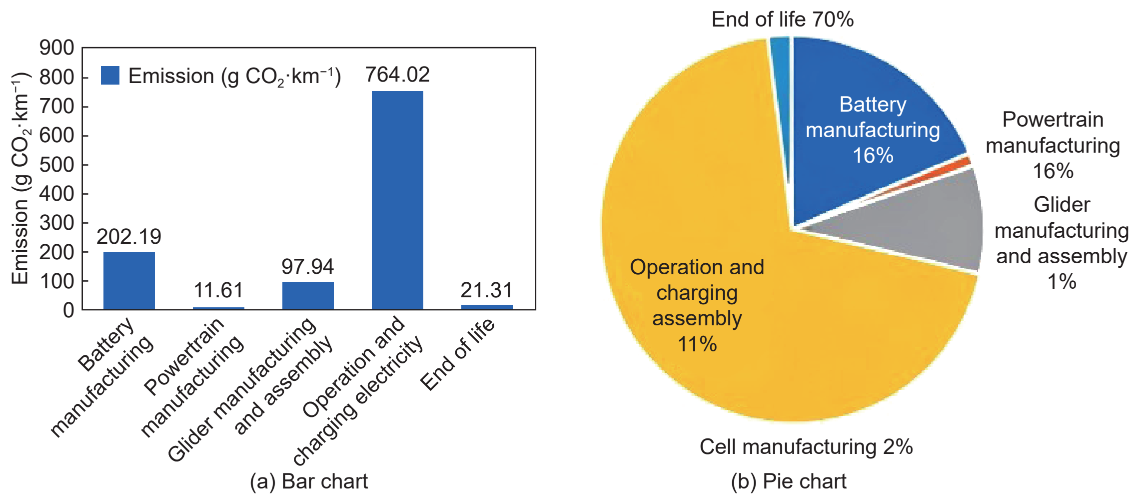

Fig. 13 Emissions in each life cycle stage chart. Reproduced with permission from Yang et al. (2024), ©Higher Education Press 2024.

hot spot in an EB's life cycle, the discussion focuses on research question 3, exploring the potential reasons behind the results (Yang et al., 2024). First, the emissions of an EB and a conventional ICE bus are compared, which reveals that electrification greatly reduces emissions. The discussion then shifts to whether and how the power grid affects the benefits of bus electrification. Finally, the effects of temperature are considered. Suggestions are proposed following each topic of discussion.

In this study, stages such as powertrain manufacturing, glider assembly, and end-of-life processes for conventional ICE buses and EBs are assumed to be identical, allowing standardization, as shown in Fig. 14. The analysis focuses solely on battery manufacturing and charging electricity for EBs versus fuel production for ICE buses, enabling clear emission comparisons between the two vehicle types (Cui et al., 2024a). Built on the model through the same approach as in Section 3.1, the inputs and outputs needed for an ICE bus are shown in Table 9.

The calculated result (Table 10) of CO_2 emissions from the operation and fuel production stage of a conventional bus is 1,359.50 g CO_2·km^{-1}, whereas that of summing battery manufacturing and charging electricity stages of an EB is 933.36 g CO_2·km^{-1}. The emission reductions resulting from electrification are 426.14 g CO_2·km^{-1} and 31.3%, respectively. This reduction in emissions highlights the environmental benefits of electrifying bus fleets. The comparative analysis reveals critical differences in lifecycle stages between EBs and conventional ICE buses. While

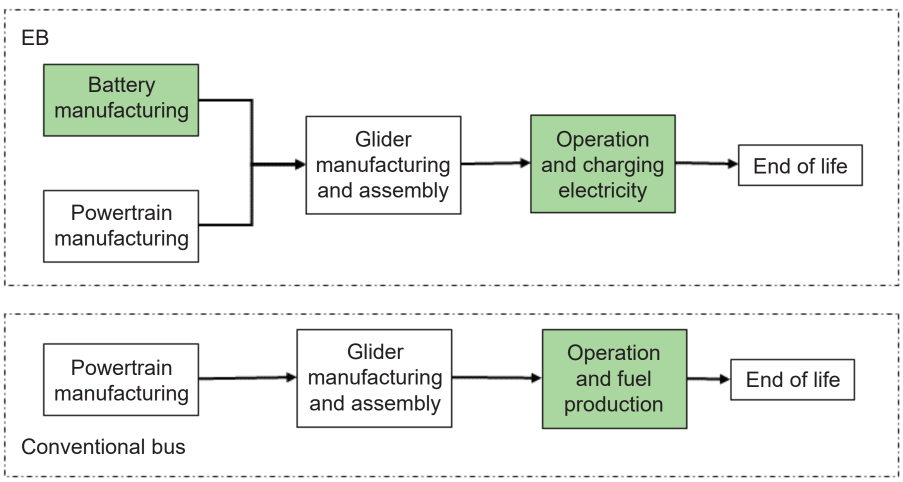

Fig. 14 Comparative flowcharts of the EB and conventional ICE buses. Reproduced with permission from Cui et al. (2024a), ©Elsevier 2024.

Table 9 Inputs and outputs for the LCI analysis of the operation and fuel production stages of the conventional bus

Data	Value	Unit	Source
		Input	
Vehicle	1	veh	Same as EB
Lifetime operation	429,824	km	Same as EB
Fuel	41.67	L·100 km^{-1}	Nilrit and Sampanpanish (2012)
		Output	
CO_2 Emissions			
From tailpipe CO_2 emissions	114.01	kg CO_2·100 km^{-1}	Nilrit and Sampanpanish (2012)
From fuel production CO_2 emissions	0.50	kg CO_2-eq·L^{-1}	Global Energy Internet Development and Cooperation Organization (2021)

Table 10 CO_2 emission comparison between EBs and conventional buses (Unit: g $CO_2 \cdot km^{-1}$)

EB		Conventional bus	
Battery manufacturing	169.34	—	
Operation and charging electricity	764.02	Operation and fuel production	1,359.50
Total	933.36	Total	1,359.50
	g $CO_2 \cdot km^{-1}$		g $CO_2 \cdot km^{-1}$

both vehicle types share equivalent powertrain manufacturing and glider assembly processes, the divergence arises from energy sourcing and end-use efficiency. For ICE buses, Table 9 highlights that over 88% of operational emissions originate from direct fuel combustion, with only 0.43% attributed to upstream fuel production. Conversely, EBs shift 71% of emissions to electricity generation and battery production (764.02 g $CO_2 \cdot km^{-1}$ from charging vs. 169.34 g CO_2 km^{-1} from batteries). This shift creates a leverage point for emission reduction through renewable energy integration in power grids—a factor not fully captured in this study owing to its reliance on the IPCC's 2006 average emission factors for grid electricity.

Notably, the 31.3% emission reduction assumes standardized battery production processes, which may underestimate material-specific impacts. For example, cathode material selection can cause ±20% variation in manufacturing emissions according to data from Argonne National Laboratory's 2022. Additionally, the 429,824 km lifetime assumption aligns with Guangzhou's operational requirements but may not reflect shorter vehicle lifespans in regions with intensive road conditions, potentially affecting total life cycle emission calculations. The reduction in emissions from EBs compared with those from conventional buses directly supports EBs.

This study demonstrates that scaling up Guangzhou's 15,000 electric buses over its 429,824 km lifespan could reduce life cycle CO_2 emissions by 2,747.5 kton, substantially lowering transportation-related emissions. While large-scale electrification of bus fleets is critical for sustainable urban mobility, regional variations in energy structures globally significantly impact life-cycle GHG emissions—fossil fuel-dependent regions exhibit far higher emissions than those using renewable energy. The next section analyzes how power grid composition influences electrification benefits on a national scale.

The results revealed that most emissions originate from the operation and charging electricity phase, which suggests that the energy used during the operation of the vehicle and the electricity sources for charging are highly carbon intensive. To determine why, it is crucial to assess the mix of energy sources in the electricity grid where EBs are charged. Guangzhou city is the capital city of Guangdong Province. Of all the province's electricity sources, one-third come from external power. The remainder is internal power, with thermal power accounting for approximately 65% of the province's installed capacity and hydropower accounting for approximately 11.7% (Guangzhou Municipal Public Security Bureau, 2018), as shown in Fig. 15.

The electrification of buses is an effective way to reduce emissions. However, regional divergence needs to be considered. Fig. 16 shows such divergence USA, which is measured as the EB fraction of the ICEB lifetime CO_2 emissions. A value less than 1 indicates that the EB is preferred in terms of its environmental impact (Koech et al., 2024).

Regional divergence can also directly influence the preference for EBs in China and demonstrated by the indicator of carbon emission intensity of electricity generation (CEIE) (Cui et al., 2024b; Sun et al., 2023; Zhang et al., 2020). Since Guangzhou city is one of the most developed cities in China, the area of

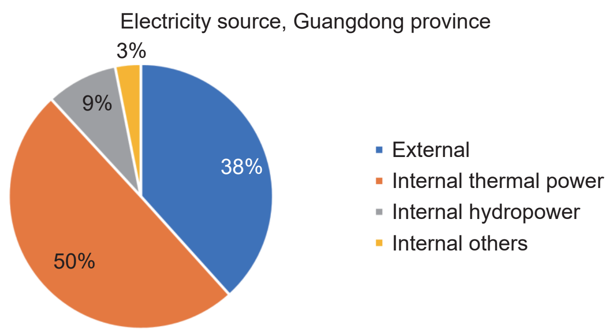

Fig. 15 Electricity sources in Guangdong province.

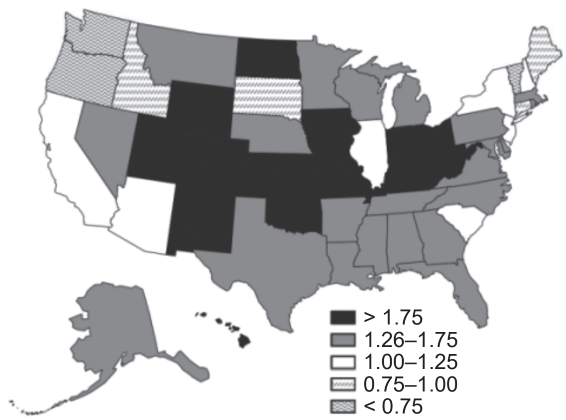

Fig. 16 State-by-state preference for EB or ICEB accounting for electric grid differences in USA.

Guangzhou city is located at the middle level of CEIE, i.e., $(500–700)\times10^6$ t·kWh^{-1}. Considering that there are still other cities, especially the regions distributed in Northeast China and North China, that feature higher CEIE and fewer green electricity generation approaches or are facing difficulties in building adequate and technically proper charging infrastructure for EVs. For those areas, apart from developing a greener power grid, it is still important to develop and innovate in conventional vehicles.

China aims to peak CO_2 emissions by 2030 and advance net-zero goals through accelerated development of renewable energy, particularly large-scale and high-quality wind and solar power projects. This strategy emphasizes both centralized and distributed energy systems while prioritizing the construction of wind and photovoltaic power bases to reduce fossil fuel reliance. Therefore, based on the same prediction model (Zhang et al., 2023) as the EF used earlier, when the carbon peak reaches 2030, the EF will be 0.7363. The calculation reveals that there will be a significant reduction in CO_2 emissions, 167.64 g $CO_2 \cdot km^{-1}$, between the LCA results in 2021, as above, and those in 2030, as shown in Table 11.

Noticeably, the emission from every stage is reduced (Fig. 17). The reduction in emissions for operation and charging electricity is the greatest, by 100.25 g $CO_2 \cdot km^{-1}$ and 13.12%, respectively, followed by that for battery manufacturing, which is 42.37 g $CO_2 \cdot km^{-1}$ and 20.85%, respectively. However, even though the reduction at the end-of-life stage is as high as 27.17%, the absolute

Table 11 CO_2 emissions corresponding to EFs in 2021 and 2030 and their reduction

Life cycle stage	Emission (g CO_2-eq·km^{-1})			Reduction rate
	2021	2030	Reduction	
Battery manufacturing	202.19	159.82	42.37	20.95%
Powertrain manufacturing	11.61	9.19	2.42	20.83%
Glider manufacturing and assembly	97.94	81.12	16.82	17.17%
Operation and charging electricity	764.02	663.77	100.25	13.12%
End of life	21.31	15.52	5.79	27.17%
Total	1,097.07	929.43	167.64	15.28%

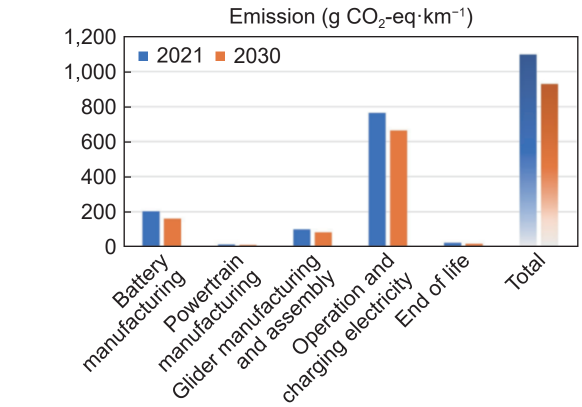

Fig. 17 Emission comparison between 2021 and 2030. Reproduced with permission from Zhang and Xu (2023), © Elsevier 2023.

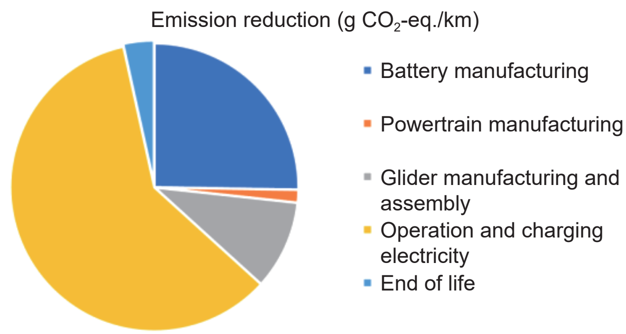

Fig. 18 Proportions of emission reduction in different stages of the total reduction from 2021 to 2030. Reproduced with permission from Zhang and Xu (2023), © Elsevier 2023.

reduction is only 5.79 g CO_2·km^{-1} (see Fig. 18). However, even with the anticipated improvements in the power grid by 2030, which are expected to further reduce emissions due to greener electricity sources, the slight reduction in emissions from EBs is projected to be only 167.64 g CO_2·km^{-1}.

The EF used in the LCA is from China's southern power grid, 0.8475, which is much greater than Singapore's 0.4085, Sweden's 0.027. The local power grid is relatively carbon intensive. This is also reflected by the electricity generation sources in these three countries (see Table 12 and Fig. 19). Clearly, more than 60% of electricity was generated from coal in 2021, while the majority of electricity generation sources in Singapore were wind, and Sweden mainly used nuclear and hydro energy. The impact of the electricity grid on the sustainability performance of EBs is a complex issue. The results of the analysis clearly indicate that the electricity charging phase of EBs results in the highest emissions, largely because of the high carbon intensity of the local electricity grid.

Section 4.2 reveals the carbon intensity of the local power grid as a main cause of high emissions during EB operation and

Table 12 Proportions of electricity generation sources in China, Sweden, and Singapore in 2021

Electricity generation sources	China	Sweden	Singapore
Coal	63.0000%	0.43%	1.19%
Oil	0.1300%	0.20%	0.99%
Nature gas	3.1200%	0.16%	93.93%
Nuclear	4.7400%	30.83%	—
Hydro	15.5700%	43.03%	—
Tide	0.0001%	—	—
Biofuels	1.9000%	6.56%	0.51%
Waste	0.0800%	2.03%	2.09%
Wind	7.6300%	15.86%	—
Solar PV	3.8000%	0.89%	1.30%
Solar thermal	0.0200%	—	—
Geothermal	0.0015%	—	—

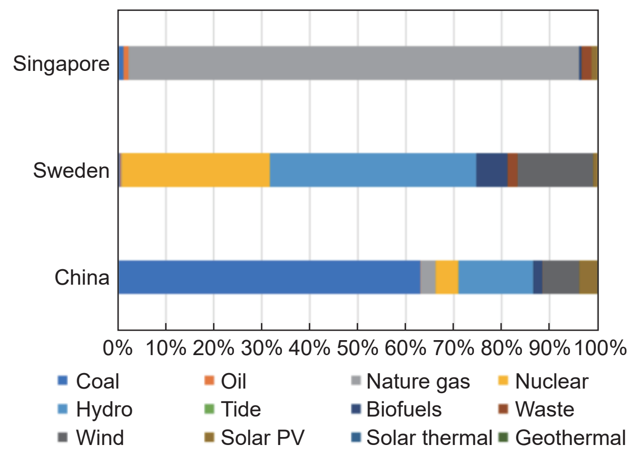

Fig. 19 Proportions of electricity generation sources in China, Sweden, and Singapore in 2021.

charging in its life cycle and highlights regional differences in China's carbon intensity. Moreover, by 2030, when China reaches its carbon peak with a lower EF, the reduction in an EB's life cycle CO_2 emissions is minimal. Moreover, it compared China's grid with others, confirming that it is far from optimal. Combined with the analysis of the benefits of electrifying the bus fleet for CO_2 emissions, Section 4.2 concludes that due to regional and global power grid differences, universal public bus electrification is not the sole sustainable solution in the automotive industry. This represents a single approach among many for reducing emissions. Thus, tailored regional strategies are needed. In areas with green grids, electrification helps mitigate CO_2 emissions, whereas in carbon-intensive grid areas, policies should focus on cleaner electricity. Moreover, more comprehensive strategies involving technological progress, such as improving hybrid vehicle performance, enhancing energy efficiency, and promoting renewable energy, should be considered. Meeting these requirements will make substituting conventional buses with EBs truly beneficial.

When processing the data, many bus trips with similar trip durations but dissimilar energy consumption rates were noted. There could be many factors behind this phenomenon: (1) Frequency of braking and acceleration. Vehicles in general consume less energy when operating in a steady state than when constantly braking and accelerating. The choice of bus lanes must be considered. Most bus operation lanes in the city of Guangzhou are hybrid lanes; these lanes are dedicated only to bus lanes from 7:00 AM to 7:00 PM. In addition to these hours, the lanes are shared-use bus lanes that also allow regular vehicles. Energy consumption will be greater in shared-use bus lanes, especially in traffic congestion (Sun et al., 2024). Bus routes that focus on dedicated bus lanes tend to consume less energy than routes that focus on hybrid or share-used bus lanes. (2) Different battery types. The field data used in this study only separate buses by different bus ID and trip ID. Exactly which bus model/brand is used for which route is unknown, along with the type of battery and its nominal capacitance. One can make an educated guess on one of the potential reasons for some trips for similar bus routes with the same service type and similar operation times consuming relatively different amounts of energy, which could be that the buses use different batteries with different weights and nominal capacities. Battery packs that weigh more will add more weight to the bus itself and consume more energy to power. (3) Differences in regional topography. The topography of Guangzhou city is relatively high and hilly in the northeast, with an altitude of 1,210 m, and lower in the southwest. The northern and northeastern areas are mountainous areas, and the southern area is an alluvial plain of the Pearl River Delta. The central part is a hilly basin, while the urban area has Baiyun Mountain. The energy consumption will be greater when buses operate in mountain areas where there are many sharp turns and up-and-downs on the bus route and lower when operating on a relatively flat and smooth route. (4) Traffic condition. Despite the attempt to offset the influence of peak hours in this study, different buses operating in different parts of the city where traffic conditions are different will lead to minor differences in energy consumption. (5) Ambient temperature. EV batteries have an optimal operating window with respect to ambient temperature. Within this window, the energy consumption is the lowest when all other factors are equal. The energy consumption of morning-only bus trips tends to be lower than that of afternoon-only bus trips, as in most cases, the ambient temperature in the morning is lower than that in the afternoon.

This section investigates the impact of ambient temperature on energy consumption in electric buses via CAN and GPS data from a single bus (No. 497) operating in Guangzhou during May 2021. Ambient temperature fluctuations alter battery resistance, affecting total energy use, whereas extreme temperatures increase the air conditioning demand. Table 13 shows that the data spanned 131 trips recorded every second, with ambient temperatures ranging from 21 to 37.5 °C (excluding nighttime trips). To isolate temperature effects, rush-hour trips (7:00–9:00 AM and 5:00–7:00 PM) were excluded on the basis of Guangzhou's traffic regulations. Energy consumption for each trip was calculated via Eq. (13) to account for trip duration, initial/final battery state-of-charge (SoC), and hourly temperature data from Global Energy internet Development and Cooperation Organization (2021). Trips were grouped into 3.9 °C intervals (e.g., 21–23.9 °C) to mitigate measurement errors caused by delayed SoC readings. The dataset, sorted by trip start/end times and temperature, revealed average trip durations of 23 min and 15 s. This approach ensures robust analysis of temperature-driven energy variations while addressing data limitations. Fig. 20 is an example of an expected SoC (blue line) that decreases as the bus continues to operate. Fig. 21 shows an example of fluctuating SoC values being read by the battery level meter on the bus; the value

Table 13 Example of singular trip data with hourly temperature information

Date	Triplog ID	Begin	End	Duration	SoC initial	SoC final	E (kWh)	Temp (°C)
May 02	915 193 375	08:35:00	08:53:00	00:18:00	100	97	10.113	26.5
	915 205 130	09:00:00	09:25:00	00:25:00	97	95	6.742	27.5
	915 216 077	10:00:00	10:23:00	00:23:00	95	92	10.113	29
…	…	…	…	…	…	…	…	…
May 31	927 403 348	09:00:00	09:24:30	00:24:30	97	95	6.742	30
…	…	…	…	…	…	…	…	…

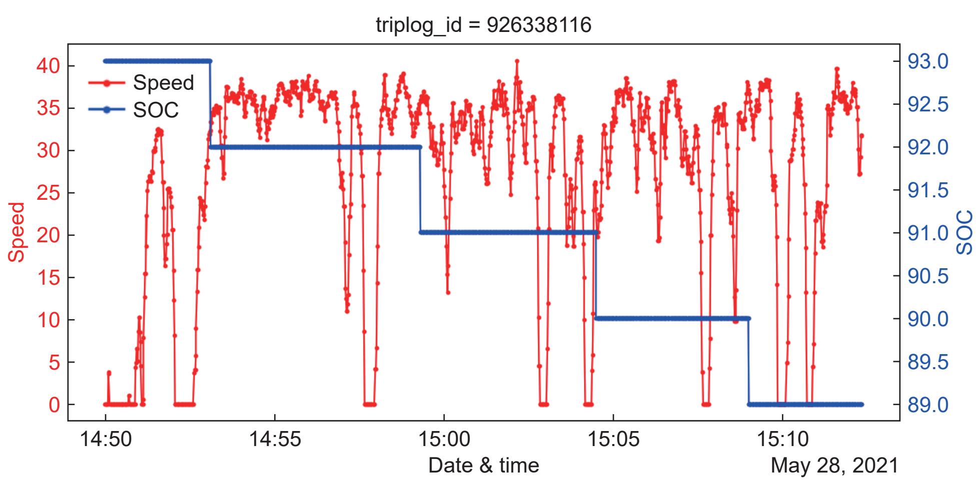

Fig. 20 Example of expected SoC behavior.

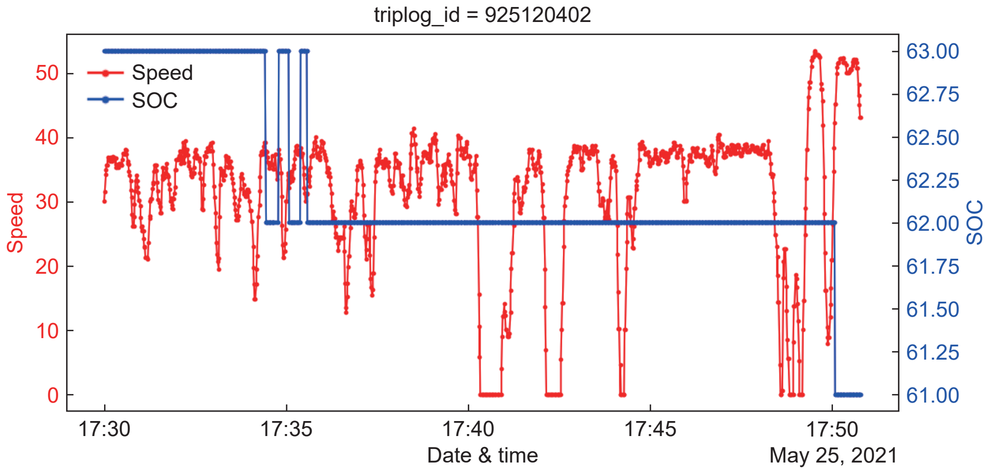

Fig. 21 Example of delayed SoC behavior.

jumps between 63% and 62% at approximately 5:35 PM.

The average energy consumption per trip of the 6 bus groups was calculated separately and then divided by the average mileage per trip to obtain the average specific energy consumption under different ambient temperatures, as shown in Table 14. From the graph in Fig. 22, for bus ID = 497 running on the same route, the per-trip energy consumption is lowest at approximately 22–23 °C and increases when the temperature exceeds 22 °C. Morning`s first trip usually has the lowest ambient temperature during bus operation, and owing to the faster initial battery discharge speed at 100% SoC, its energy consumption is higher, making the theoretical per-trip energy consumption value slightly lower than the calculated value. Despite this small error, it is clear that the average per-trip energy consumption increases with increasing ambient temperature.

According to China's annual average temperature map from Top China Travel, the middle east part of China generally has the most suitable temperature range for electric vehicles, yet the CEIE is quite high, so policymakers should prioritize promoting electric buses and making energy cleaner in this area. Guangdong Province has a lower CEIE than some other regions do, but since Guangzhou (with the highest annual average temperature in China) has a higher specific energy consumption for electric buses than most regions in the country do, efforts in this region should focus on cleaner energy production for improvement.

Table 14 Average energy consumption per trip for different ambient temperature trip groups

Temperature group (°C)	Average energy consumption (per trip·kWh^{-1})
21.0–23.9	6.74
24.0–26.9	8.43
27.0–29.9	8.85
30.0–32.9	8.99
33.0–35.9	9.23
36.0–38.9	9.69

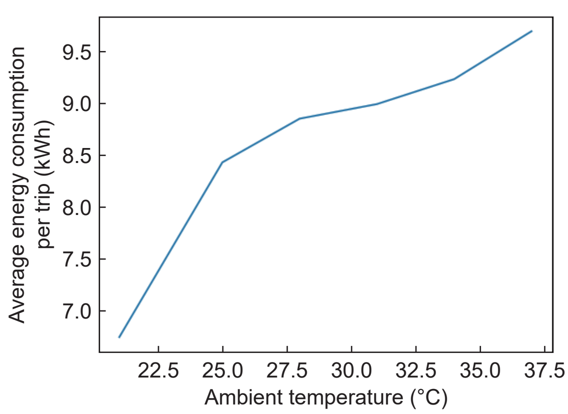

Fig. 22 Average energy consumption per trip at the different ambient temperatures. Reproduced with permission from Yang et al. (2024), ©Higher Education Press 2024.

4.3 Limitations

Even though our study uses field data during operation obtained from a city in China, other datasets of battery production and powertrain manufacturing would only be found through existing studies, instead of being obtained directly from a production company. Such data inevitably lead to slight inaccuracies due to temporal and regional discrepancies. This study is subject to the following key limitations, which may influence the generalizability and precision of the results:

1) Regional data constraints

The field data were geographically confined to Guangzhou. This restricts their applicability to cities with similar climates and operational patterns.

2) Battery production data limitations

Manufacturing data for batteries and powertrains relies on existing studies, introducing potential discrepancies due to technological evolution and regional production variances.

3) Incomplete environmental variables

Ambient temperature impact analysis overlooks interactions with humidity, wind speed, and air pressure fluctuations.

4) Assumption sensitivities

The 31.3% emission reduction assumes static battery chemistry, whereas emerging LFP batteries could alter manufacturing emissions by ±15% (Argonne National Lab, 2022).

5 Conclusions

This study assessed the life cycle CO_2 emissions of electric buses in Guangzhou via LCA, with a focus on stages from manufacturing to disposal. Field data combined with government and academic sources were analyzed to quantify emissions, prioritizing variables such as speed patterns and charging intervals. The results revealed that operational energy use dominated, driven by Guangzhou's carbon-intensive grid. While EBs have lower emissions than conventional ICE buses do, regional grid variability necessitates renewable energy integration and smart grid adoption for significant reductions.

清華大学出版社 Tsinghua University Press | Available on IEEE Xplore®

The data used in this study were collected over a short period, which may not fully represent the annual variation in energy consumption and emissions. Additionally, the study focused on a localized area in Guangzhou and did not account for the diversity of electric bus models and battery types, which could influence the results. The accuracy and completeness of the field data, as well as potential biases in the data sources, also pose challenges to the generalizability of the findings.

To address these limitations and guide future research, several specific directions are proposed. First, improving data collection methods is crucial. This can be achieved by utilizing more advanced and continuous data monitoring systems, increasing the frequency and duration of data collection, and ensuring the accuracy and completeness of the data through rigorous validation processes. Second, expanding the scope of research is essential. Future studies should cover a wider range of regions with different climatic conditions and grid structures and include various types of electric buses and battery technologies to increase the robustness and generalizability of the results. Finally, incorporating additional factors such as detailed battery degradation models, regional policies, and socioeconomic impacts will further enrich the analysis. This study proposes two focused future research directions: validating the LCA model in cities with contrasting grid structures and correlating real-time temperature data with energy consumption patterns to optimize charging schedules.

Replication and data sharing

The program code used within this research can be made accessible upon request via email to the corresponding author.

Acknowledgements

This research was supported by the National Natural Science Foundation of China (No. 52372313) and JPI Urban Europe and Energimyndigheten (No. e-MATS, P2023–00029).

Declaration of competing interest

The authors have no competing interests to declare that are relevant to the content of this article.

References

Abdelwahab, S. H., Alhasheem, M., Sharkawy, R. M., 2024. Optimization for charging scheduling in electric bus system. In: 2024 6th International Youth Conference on Radio Electronics, Electrical and Power Engineering (REEPE), 1–6.

Chen, Q., Lai, X., Gu, H., Tang, X., Gao, F., Han, X., et al., 2022. Investigating carbon footprint and carbon reduction potential using a cradle-to-cradle LCA approach on lithium-ion batteries for electric vehicles in China. *J Clean Prod*, **369**, 133342.

Cui, S., Xue, Y., Gao, K., Wang, K., Yu, B., Qu, X., 2024a. Delay-throughput tradeoffs for signalized networks with finite queue capacity. *Transp Res Part B Methodol*, **180**, 102876.

Cui, S., Xue, Y., Lv, M., Gao, K., Yu, B., Cao, J., 2025. Temporal finite-time adaptation in controlling quantized nonlinear systems amidst time-varying output constraints. *IEEE Trans Autom Sci Eng*, **22**, 3265–3279.

Cui, S., Yang, Y., Gao, K., Cui, H., Najafi, A., 2024b. Integration of UAVs with public transit for delivery: Quantifying system benefits and policy implications. *Transp Res Part A Policy Pract*, **183**, 104048.

Eufrásio., Daniel, J., Delgado, O., 2023. Operational Analysis of Battery Electric Buses in São Paulo. International Council on Clean Transportation(ICCT). https://theicct.org/wp-content/uploads/2023/02/Operational-analyis-of-battery-electric-buses-in-Sao-Paulo-final-feb2023.pdf

Fallah, N., Fitzpatrick, C., 2023. Is shifting from Li-ion NMC to LFP in EVs beneficial for second-life storages in electricity markets? *J Energy Storage*, **68**, 107740.

Guangzhou Municipal Public Security Bureau, 2018. Guangzhou motor vehicle service life standards and scrapping Procedure instructions. http://www.gz.gov.cn/gzgov/s5812/201809/ae562c2c6bf24841b2d9c-518c84b4cec.shtml

Hauschild, M. Z., Rosenbaum, R. K., Olsen, S. I., 2018. *Life Cycle Assessment: Theory and Practice*. Cham, Switzerland: Springer International Publishing.

Karabacak, Y., Ali Ozkan, İ., Sarİtas, İ., 2020. Estimation of li-ion battery state of charge using adaptive neural fuzzy inference system (ANFIS). *Int J Energy Appl Technol*, **7**, 88–94.

Koech, M. C., Fahimi, B., 2024. An energy demand analysis and emission reduction potential of electric buses for cities in developing economies: A case study of Nairobi, Kenya. In: 2024 IEEE PES/IAS PowerAfrica, 1–5.

Li, J., Li, L., Yang, R., Jiao, J., 2023. Assessment of the lifecycle carbon emission and energy consumption of lithium-ion power batteries recycling: A systematic review and meta-analysis. *J Energy Storage*, **65**, 107306.

Liu, F., Shafique, M., Luo, X., 2024. Unveiling the determinants of battery electric vehicle performance: A systematic review and meta-analysis. *Commun Transp Res*, **4**, 100148.

Lin, H., Liu, Y., Wang, L., Qu, X., 2025. Big data-driven advancements and future directions in vehicle perception technologies: From autonomous driving to modular buses. *IEEE Trans Big Data*, **11**, 1568−1587.

Liu, Y., Wu, F., Liu, Z., Wang, K., Wang, F., Qu, X., 2023. Can language models be used for real-world urban-delivery route optimization? *Innovation*, **4**, 100520.

Majeau-Bettez, G., Hawkins, T. R., Strømman, A. H., 2011. Life cycle environmental assessment of lithium-ion and nickel metal hydride batteries for plug-In hybrid and battery electric vehicles. *Environ Sci Technol*, **45**, 4548−4554.

Notter, D. A., Gauch, M., Widmer, R., Wäger, P., Stamp, A., Zah, R., et al., 2010. Contribution of Li-ion batteries to the environmental impact of electric vehicles. *Environ Sci Technol*, **44**, 6550−6556.

Nordelöf, A., Romare, M., Tivander, J., 2019. Life cycle assessment of city buses powered by electricity, hydrogenated vegetable oil or diesel. *Transp Res Part D Transp Environ*, **75**, 211−222.

Ritchie, H., 2020. Cars, planes, trains: where do CO_2 emissions from transport come from our world in data. https://ourworldindata.org/co2-emissions-from

Argonne National Lab., Meisterling, K., 2022. Life cycle assessment of greenhouse gas emissions from plug-in hybrid vehicles: Implications for policy. *Environ Sci Technol*, **42**, 3170−3176.

Sistig, H. M., Sinhuber, P., Rogge, M., Sauer, D. U., 2025. Evaluating costs and operations of public bus fleet electrification. *NPJ Sustain Mobil Transp*, **2**, 15.

Shui, B., Shafique, M., Luo, X., 2024. Light-duty passenger vehicle electrification in China from 2021 to 2050 and associated greenhouse gas emissions: A dynamic fleet perspective. *Transp Res Part D Transp Environ*, **130**, 104199.

Sun, S., Batista, S. F. A., Menéndez, M., Wang, Y., Zhang, S., 2024. Powering up urban mobility: A comparative study of energy efficiency in electric and diesel buses across various lane configurations. *Sustain Cities Soc*, **101**, 105086.

Sun, X., Lian, W., Gao, T., Chen, Z., Duan, H., 2023. Spatial-temporal characteristics of carbon emission intensity in electricity generation and spatial spillover effects of driving factors across China's provinces. *J Clean Prod*, **405**, 136908.

Top China Travel, 2004. Average annual temperature map of China. https://www.topchinatravel.com/China-map/average-annual-temperature-map-of-China.html

Yang, Y., Cheng, J., Liu, Y., 2024. An overview of solutions to the bus bunching problem in urban bus systems. *Front Eng Manag*, **11**, 661–675.

Yang, Y., Tian, G., Li, F., Jia, T. X., Wang, X. H., Huang, X. D., 2023. Application scenario analysis and prospect of electricity emissions factor. In: 2022 12th International Conference on Power and Energy Systems (ICPES), 697–703.

Zhang, M., Lv, T., Zhao, Y., Pan, J., 2020. Effectiveness of clean development policies on coal-fired power generation: An empirical study in China. *Environ Sci Pollut Res Int*, **27**, 14654–14667.

Zhang, X., Xu, K., 2023. Statistical data-based prediction of carbon dioxide emission factors of China's power generation at carbon peak in 2030. *Case Stud Therm Eng*, **51**, 103633.

Baozhen Yao received the Ph.D. degree from Beijing Jiaotong University in 2011 and is currently a Professor and doctoral supervisor at the School of Mechanical Engineering at Dalian University of Technology. Her research interests focus on vehicle-road collaboration systems, intelligent connected vehicles (ICVs), and intelligent transportation systems (ITSs).

Zhihao Qi is currently pursuing the M.S. degree in vehicle engineering at the School of Mechanical Engineering, Dalian University of Technology. His research focuses on perception-oriented technologies in intelligent driving systems, particularly in terms of exploring sensor fusion algorithms and understanding the driving environment.

Ziqi Liu received the B.S. degree from Tongji University and the M.S. degree from Chalmers University of Technology in 2025. Her research focuses on life cycle assessment and data analysis, with an emphasis on evaluating the environmental impacts of transportation systems, and utilizing data analytics for sustainability assessments.

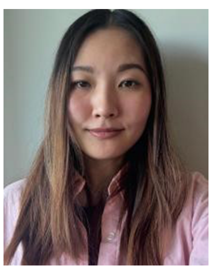

Minke Zhu received the B.S. degree from Chongqing University in 2023 and the M.S. degree from Chalmers University of Technology in 2025. Her research interests include electrification technologies and data analysis, with a focus on developing efficient methodologies for electric vehicle systems, and applying data-driven approaches for performance evaluation and optimization.

Shaohua Cui is currently a postdoctoral researcher with the Urban Mobility Systems Research Group, Department of Architecture and Civil Engineering, Chalmers University of Technology (CTH). He received the M.S. degree from the systems science institute, School of Traffic and Transportation, Beijing Jiaotong University, in 2019 and the Ph.D. degree in transportation engineering from Beihang University in 2023. His research interests include traffic flow analysis, vehicle control, adaptive control, and robust control.

Radu-Emil Precup received the Dipl.Ing. (Hons.) degree in automation and computers from the Traian Vuia Polytechnic Institute of Timisoara, Timisoara, Romania, in 1987; the diploma degree in mathematics from the West University of Timisoara, Timisoara, in 1993; and the Ph.D. degree in automatic systems from the Politehnica University of Timisoara (UPT), Timisoara, in 1996. He is currently with UPT, where he became a Professor with the Department of Automation and Applied Informatics in 2000. Since 2022, he has also been a Senior Researcher (CSI) and the Head of the Data Science and Engineering Laboratory, Center for Fundamental and Advanced Technical Research, Romanian Academy Timisoara Branch, Timisoara. From 2016 to 2022, he was an Adjunct Professor with the School of Engineering, Edith Cowan University, Joondalup, WA, Australia. He is the author or coauthor of more than 300 papers. His current research interests include intelligent and data-driven control systems. He is a corresponding member of the Romanian Academy. He is a member of the Technical Committees on Data-Driven Control and Monitoring and Control, Robotics and Mechatronics of the IEEE Industrial Electronics Society. He is the Editor-in-Chief of the *Romanian Journal of Information Science and Technology*, the Executive Editor-in-Chief of *Information Sciences*, and an Associate Editor/Editorial Board Member of *IEEE Transactions on Cybernetics*, *IEEE Transactions on Neural Networks and Learning Systems*, *Applied Soft Computing*, *Expert Systems with Applications*, *Engineering Applications of Artificial Intelligence*, *Evolving Systems*, *Applied Artificial Intelligence*, and *Healthcare Analytics*.

Raul-Cristian Roman received the B.S., M.S., and Ph.D. degrees in systems engineering from the Politehnica University of Timisoara (UPT), Timisoara, Romania, in 2012, 2014, and 2018, respectively. He is currently with UPT, where he became an Assistant Lecturer with the Department of Automation and Applied Informatics in 2018. He has coauthored more than 40 articles. His research interests include control structures and algorithms and optimization with a focus on data-driven control. He was a corecipient of the Best Paper Award at the 7th International Conference on Information Technology and Quantitative Management, Granada, Spain, in 2019. He is a member of the Romanian Society of Control Engineering and Technical Informatics.